

Elongation of Telechelic Ionomers under Shear: a Rheological and Rheo-optical Study

Christophe Chassenieux[†] and Jean-François Tassin*

Chimie et Physique des Matériaux Polymères, UMR CNRS 6515, Université du Maine, Avenue Olivier Messiaen, 72085 Le Mans Cedex 9, France

Jean-François Gohy and Robert Jérôme

Centre for Education and Research on Macromolecules, Institute of Chemistry B6, University of Liège, Sart Tilman, 4000 Liège, Belgium.

Received October 13, 1999; Revised Manuscript Received December 27, 1999

ABSTRACT: The behavior under shear of solutions of α,ω -lithium sulfonato polystyrene (α,ω -LiPSS100) in toluene has been investigated by rheo-optics and rheology. Shear-thickening is observed and related to a strong increase of birefringence and a pronounced and rapid alignment of the polymer chains toward the flow direction leading to an important elasticity of the fluids. The draw ratio of the polymer chains under shear has been estimated from the rheo-optical data. When the fraction of loops is taken into account, draw ratios on the order of 4 are calculated in the shear thickening regime.

Introduction

Ionomers are linear polymers containing less than 15 mol % of ionic groups.¹ Telechelic ionomers are model systems for ionomers in general since they have a low polydispersity index and their functionality is directly controlled by the molecular weight since the ionic groups are selectively located at the chain ends.²

Solution of α,ω -halato-telechelic ionomers in apolar solvents show an increase in viscosity by several orders of magnitude beyond a characteristic concentration denoted C_{gel} , by analogy with chemically cross-linked gels. It must be emphasized that C_{gel} is well below the overlap concentration of the polymer coils (C^*). It is now well established³ that this viscosity increase results from the formation of a transient network whose physical cross-links are constituted by multiplets (i.e., polar microdomains where ionic groups associate due to electrostatic interactions). Before a rather well-defined network is obtained, aggregates containing several multiplets are formed.

These solutions under oscillatory shear show a very simple Maxwell type behavior. At low frequency a liquid like behavior is observed whereas at high frequencies, the elastic modulus G' tends toward a plateau value (G_0).^{3–4} In addition, a narrow distribution of relaxation times^{3–5} is obtained. The thermorheological behavior is quite simple too: the temperature dependence of the shift coefficients agrees with an Arrhenius law.^{3–4} The relaxation of a macroscopic strain is therefore controlled by the thermal stability of the multiplet rather than by the conformational relaxation of the chain segments.

In contrast, the steady-shear properties are relatively complex. Solutions often exhibit shear-thickening and shear-thinning.^{5–7} As for other associative polymers, the rheological features of the transient network formed in solutions make ionomers useful as rheology modifiers.

This paper aims at reporting on nonlinear rheology and rheo-optical behavior of solutions in toluene of a

high molar mass polystyrene end-capped by lithium sulfonato groups (α,ω -LiPSS100). The associative properties of this polymer were analyzed using dynamic mechanical analysis (DMA), static (SLS), and dynamic (DLS) light scattering and discussed elsewhere.³ These experimental data have suggested a relatively simple model for the association of this polymer. At low concentrations ($C < 0.01$ g/L), the polymer chains organize themselves into well-defined reversed micelles. Back-folding being observed to some extent, these micelles were referred to as flowers. For $C > 0.2$ g/L, the flowers associate into larger aggregates according to an open association mechanism. At $C_{\text{gel}} = 10$ g/L, the aggregates fill the whole space, and a transient network is formed, most likely by a percolation process. G_0 remains, however, very low indicating that only part of the aggregates contribute to the network which thus contains dangling chains and loops. As the concentration increases further, more and more aggregates become part of the network and G_0 increases rapidly ($G_0 \propto C$) until all the chains are elastically active. However, the average relaxation time obtained from oscillatory shear measurements (τ_v) does not depend on the concentration, which suggests a relatively stable conformation of the multiplets in the whole concentration range under investigation (from 10 to 17 g/L).

In this paper, the nonlinear steady-state behavior of solutions of α,ω -LiPSS100 in toluene as studied by classical rheometry and flow birefringence measurements will be presented and discussed.

Experimental Section

Materials. α,ω -Lithium sulfonato polystyrene (α,ω -LiPSS100) was synthesized by living anionic polymerization of styrene as described elsewhere.⁸ The molar mass ($M_w = 90 \times 10^3$ g/mol), the polydispersity index ($I = 1.4$) and the end-functionality ($f \approx 100\%$) were measured by size exclusion chromatography in THF.³ M and I were determined thanks to the precursor (PS100) of the telechelic polystyrene. Solutions were obtained in spectroscopic grade toluene.

Preparation of the Solutions. Time-Dependent Behavior. As already reported by several authors,^{3,7,9–10} the

* To whom correspondence should be addressed.

[†] Current address: LPM ESPCI, UMR CNRS 7615, 10 rue Vauquelin, 75231 Paris Cedex 05.

behavior of ionomer solutions may change with their aging time, leading to problems with the reproducibility of the experiments. This phenomenon becomes critical at high concentrations (for instance an equilibrium situation is reached only after 1 year for α,ω -LiPSS100 at $C = 26$ g/L). The origin might be partly found in the a relatively high value of the viscoelastic average relaxation time ($\tau_v = 20$ ms) which is directly correlated to the lifetime of an ionic group inside a multiplet.³ Therefore, to collect reliable data independent of the "history" of the sample, only solutions of relatively low concentrations (slightly above or below C_{gel}) were studied, and only stabilized solutions (no further change upon aging) were studied.

Moisture Content. Recently, Bhargava and Cooper⁵ have pointed out that moisture adsorption could modify the properties of ionomer solutions. Therefore, all the solutions were saturated with water in this study, which also contributed to the reproducibility of the measurements once the solutions were equilibrated with time.

Rheological Measurements. Steady-shear rheological data were collected with a stress-controlled rheometer (Haake RS-100) equipped with a cone and plate geometry (60 mm diameter; 1° angle) and a specific device preventing solvent evaporation. Measurements were taken with the solution at "equilibrium" under shear, based on the condition that the time evolution of the shear rate was smaller than 2%/s. If this condition was not reached, a limiting time of 2 min was chosen to avoid too long measurements. All the solutions were presheared for 10 min at $\dot{\gamma} = 1$ s⁻¹ prior to measurements, which were done at 20.0 ± 0.2 °C.

Rheo-optical Measurements. A Couette cell was used with light propagating along the vorticity axis to generate the shear flow. The radius of the inner cylinder was 15 mm, the gap was 1.5 mm and the optical path length was 24 mm.

Rheo-optical measurements were carried out using a Rheometrics Optical analyzer (ROA), operating with an He-Ne laser ($\lambda = 632.8$ nm). This equipment allows several properties of the complex refractive index tensor of the material under flow to be characterized using a polarization modulation method.¹¹ Polarization is modulated by a 2 kHz rotating half-wave plate, and the in phase and out of phase components of the modulated light intensity after passing through the sample are separated using a two phases lock-in amplifier. The signals are used to calculate the birefringence (Δn) of the sample under flow (in the velocity-velocity gradient plane) and the orientation angle χ , which defines the orientation of the principal axes of the refractive index tensor with respect to the flow direction.¹¹

Using this geometry, the optical measurements (Δn and χ) can be related to the shear stress σ_{12} and the first normal stress difference (N_1) by the stress optical laws,¹² provide they are verified.

$$\sigma_{12} = \frac{1}{2C_{so}} \Delta n \sin 2\chi \quad (1)$$

$$N_1 = \sigma_{11} - \sigma_{22} = \frac{1}{C_{so}} \Delta n \cos 2\chi \quad (2)$$

C_{so} is the so-called stress-optical coefficient which depends on the polymer chemical structure through the polarizability of the monomer units.¹³

As for the rheological measurements, all solutions were presheared for 10 min at $\dot{\gamma} = 1$ s⁻¹ prior to measurements at 20.0 ± 0.2 °C.

The absence of dichroism was checked for all of the solutions so that the presence of large aggregates in the sheared solution is unlikely and the birefringence is mainly due to the intrinsic birefringence which probes the orientation of the chain segments inside the medium. Furthermore, the transmitted intensity remained constant throughout the measurements over the various shear rates, indicating no change in the turbidity of the solutions under flow.

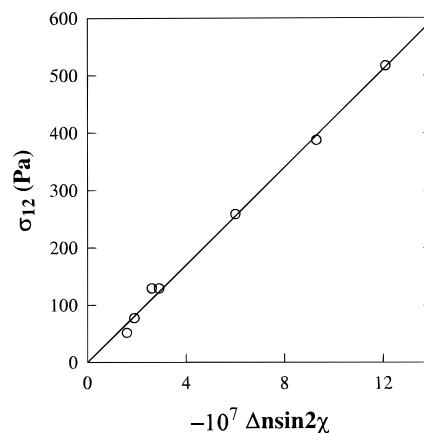


Figure 1. Shear stress vs $(-\Delta n \sin 2\chi)$ for the 400 g/L PS solution in toluene. The straight line through the experimental data validates the stress-optical law for this system.

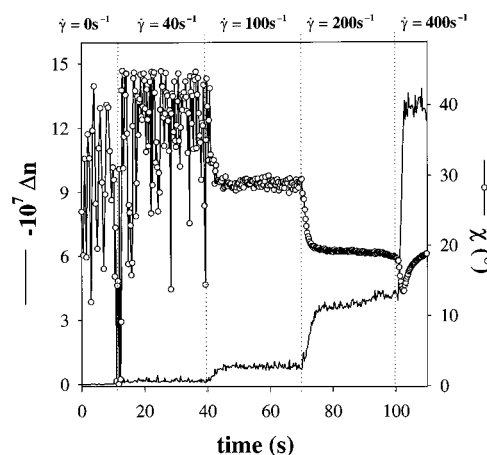


Figure 2. Time dependence of the birefringence and orientation angle at various shear rates for the $C = 12$ g/L solution of α,ω -LiPSS100 in toluene.

Results

Characterization of the Precursor. A highly concentrated solution ($C = 400$ g/L) of PS100 in toluene was prepared and characterized for the purpose of being a reference of comparable viscosity for the much less concentrated solutions of α,ω -LiPSS100. The birefringence was measured at a steady state under various shear rates. A linear increase of Δn with respect to $\dot{\gamma}$ was observed whereas the extinction angle remained equal to 45° , showing no preferential orientation of the chain segments along the flow direction. This behavior is the optical signature of a Newtonian behavior. Indeed, the solution is newtonian and with a viscosity (η) equal to 0.65 Pa·s. At a given shear rate the corresponding shear stress (σ_{12}) can thus be calculated and the validity of the stress-optical law can be checked by plotting σ_{12} vs $\Delta n \sin 2\chi$ according to eq 1 (Figure 1). The slope of the least-squares fit of the data leads to $C_{so} = -4.8 \times 10^{-9}$ Pa⁻¹. Negative values of Δn and C_{so} are expected for PS, because of the dominant contribution of the benzene rings to the polarizability and their orientation with respect to the chain axis. The value of C_{so} is in good agreement with other reported data.^{11,12}

Effect of Functionalization. Figure 2 illustrates the typical time dependence of the angle of orientation and the birefringence at various shear rates applied to a 12 g/L solution of α,ω -LiPSS100. The response of the sample to each change of shear rate is not instant-

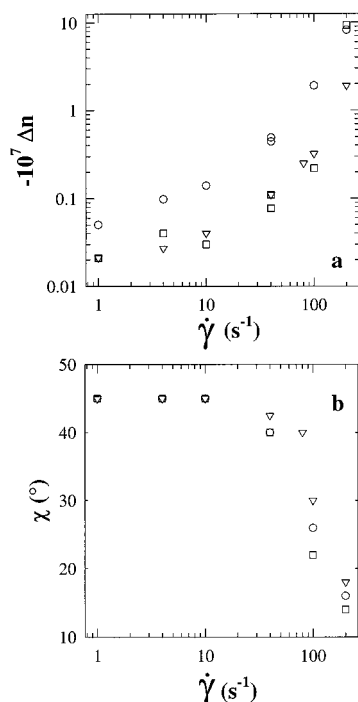


Figure 3. Shear rate dependence of the birefringence (a) and the orientation angle (b) for solutions of α,ω -LiPSS100 in toluene at $C = 8$ g/L (squares), 10 g/L (triangles) and 12 g/L (circles).

neous, and many shear units (about 50) are required to reach a steady state. Taking into account the relaxation time measured by linear viscoelasticity, this long transient state suggests a rearrangement of the system over large length scales. As the shear rate is increased, the absolute value of the birefringence increases as was the case for pure PS, whereas the angle of observation decreases sharply. This observation results from the increasing orientation of the chains in a direction parallel to the flow. Measurements at high shear rates (400 s⁻¹) are usually a problem because of a Weissenberg effect. The solution is indeed climbing out of the Couette cell, which leads to the formation of bubbles and yields a poor optical signal. This effect indicates that the α,ω -LiPSS100 solutions are highly elastic in contrast to the concentrated solution of PS which is more viscous and does not exhibit any Weissenberg effect.

Effect of Concentration. Figure 3 shows the shear rate dependence of the birefringence (Figure 3a) and of the orientation angle (Figure 3b) at three concentrations of α,ω -LiPSS100 in toluene. At the lowest shear rates, from 8 to 12 g/L, the birefringence increases by at least a factor of 4 whereas the number of objects in solution increases only by 25%.

Depending on the shear rate, two regimes can be discriminated. Below a characteristic shear rate ($\dot{\gamma}_B \approx 80$ s⁻¹), $|\Delta n|$ is proportional to $\dot{\gamma}$, which can be attributed to a "Newtonian" behavior of the solutions in terms of their birefringence. At very low shear rates, the large scale inhomogeneities within the solution that were already probed by DLS³ could account for some irregularities in the data. Above $\dot{\gamma}_B$, the birefringence increases more rapidly than the shear rate: $|\Delta n| \propto \dot{\gamma}^a$ with $a > 1$.

These two regimes are better defined when the dependence of the angle of orientation on shear rate is analyzed. At $\dot{\gamma}_B$, there is a clear transition between a regime at low shear rates where χ is constant at 45°

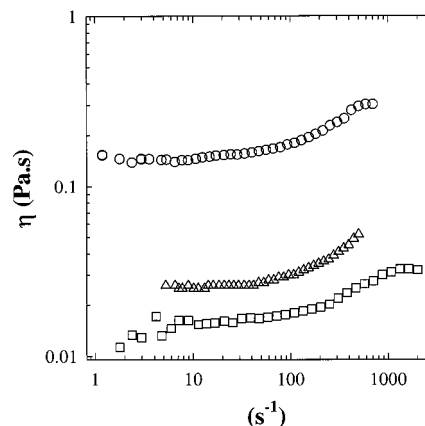


Figure 4. Shear rate dependence of the viscosity for solutions of α,ω -LiPSS100 in toluene at various concentrations (symbols are the same as in Figure 3).

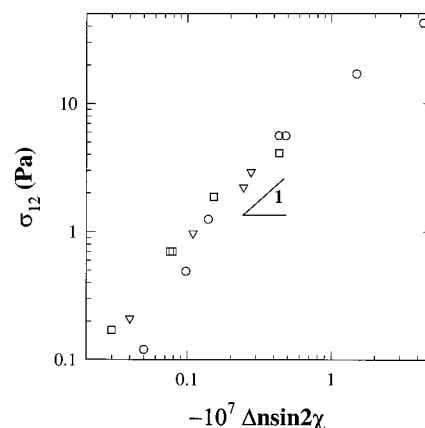


Figure 5. Shear stress vs $(-\Delta n \sin 2\chi)$ for solutions of α,ω -LiPSS100 in toluene at various concentrations (symbols are the same as in Figure 3).

and a regime at higher shear rates where χ decreases sharply as $\dot{\gamma}$ is increased. The increase of the parallel orientation of the chain with respect to the flow direction is responsible of the increasing elasticity of the fluids in qualitative agreement with the observation of a Weissenberg effect.

Comparison with Rheology. Figure 4 shows how the viscosity depends on shear rate for the same solutions of α,ω -LiPSS100 in toluene. At low shear rates, the viscosity is independent of the shear rate, consistent with a Newtonian regime. Above a characteristic shear rate ($\dot{\gamma}_V$), the viscosity of the solution increases more rapidly than the shear-rate which is the signature of a shear-thickening effect. The two characteristic shear rates $\dot{\gamma}_V$ and $\dot{\gamma}_B$ are roughly the same. However, the transition between the two regimes is smoother when observed by classical rheology rather than by rheo-optical measurements.

Another way to correlate results from rheology and rheo-optics is to check the validity of the stress-optical law. The shear stress has been plotted vs the quantity $(-\Delta n \sin 2\chi)$ in Figure 5. According to eq 1, a linear dependence indicates that the stress-optical law is fulfilled and that C_{s0} is proportional to the inverse of the slope. C_{s0} is found to be equal to -5.0×10^{-9} Pa⁻¹ in good agreement with the data obtained for unmodified PS and does not change with the concentration at least within the limits of experimental errors.

The validity of the stress optical law and the knowledge of C_{s0} allows the first normal stress difference to

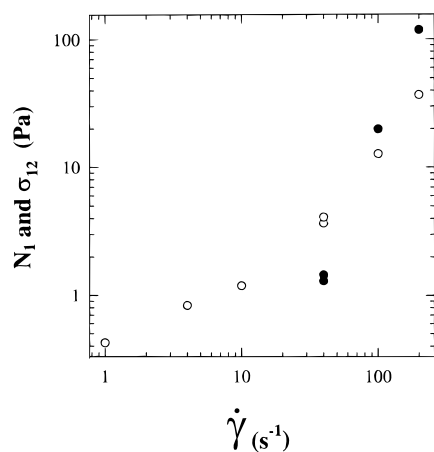


Figure 6. Shear rate dependence of the shear stress (open circles) and the first normal difference (closed circles) for the $C = 12$ g/L solution of α,ω -LiPSS100 in toluene.

be calculated from eq 2, assuming this relation is also valid. Figure 6 shows the shear rate dependence of N_1 and the shear stress for $C = 12$ g/L. At the highest $\dot{\gamma}$ values, N_1 is higher than σ_{12} , which is again an expression of the high elasticity of the solutions.

Discussion

Shear thickening of solutions of associating polymers is often although not systematically observed. This was the case for solutions of halato-telechelic polymers in nonpolar solvents⁶ and of hydrophobic ethoxylated urethanes (HEUR) in water which associate through their hydrophobic end groups.^{14,15} In these two systems, a rather regular temporary network is built up as the concentration is increased. It consists of bridges between small micelles coexisting with loops formed by chains having both of their ends trapped into the same micelle. Fluorescence measurements have shown¹⁵ that the aggregation number (at least in the HEUR system) does not change with the shear rate, suggesting that the origin of shear thickening is the stretching of the bridges connecting the micelles whereas the shear thinning would result from bridges to loops transitions. Using superposition of dynamic oscillations on steady-state flow, Tam et al.¹⁶ have observed an increase of the apparent plateau modulus in the shear thickening regime. They accounted for this observation by loop to bridge transitions, which increase the connectivity of the network. They also noted a slight decrease of the relaxation time ascribed to an easier exit of the hydrophobic groups from the micelles due the stress acting on the extended chains.

From a theoretical point of view,¹⁷ changes from intra- to interchain association as result of the chain extension have been shown to promote shear thickening¹⁸ as well as strong chain stretching inside the non-Gaussian range.¹⁹ Direct observation of chain stretching has been investigated by Pedley et al.²⁰ by small-angle neutron scattering under flow. Although shear thickening of their solutions is clearly observed, no evidence of anisotropy of the radius of gyration has been detected under flow (in the plane velocity-neutral direction). These authors have concluded that the aggregates are elongated rather than single chains

The rheo-optical data reported in this study show that shear thickening is associated with a more important increase of birefringence with shear rate as compared

Table 1. Influence of the Shear Rate on the Draw Ratio Calculated from the Birefringence Data (Eq 4) Assuming All the Chains Are Elastically Active (First Row) or Only Part of Them As Seen from the Elastic Modulus (Second Row)

concn (g/L)	draw ratio for shear rate (s^{-1})				
	40	80	100	200	
10	1.02	1.04	1.05	1.32	assuming all chains active
	1.14	1.34	1.4	2.9	assuming 1/8 of active chains
12	1.06	/	1.27	2.01	assuming all chains active
	1.25	/	2	3.7	assuming 1/4 of active chains

to the newtonian regime together with a clear decrease of the average orientation angle toward the flow direction. To quantify these effects, the draw ratio of the chains has been estimated from the birefringence data. For this purpose, it has been assumed, as a first approximation, that, under steady-state conditions, the aggregates are stretched along their principal axis by a factor λ and that the other dimension in the plane of the flow is multiplied by $1/\lambda$, the dimension along the neutral direction being unchanged.²² Deformation is supposed to be affine down to the distances between multiplets. If a chain is fully extended, the maximum birefringence reached for a solution of concentration C (w/w %) is given by

$$\Delta n = C\Delta n^0 \quad (3)$$

where Δn^0 is the so-called intrinsic birefringence of the polymer, corresponding to the fully extended chains in the melt. Its value has been determined to be -0.1 for polystyrene.²¹

Taking into account the temporary network structure of the solution and the geometry of the experiment, the optical birefringence can be written as a function of the draw ratio from classical models of rubber elasticity as²³

$$\Delta n = C\Delta n^0 \frac{1}{10N} (2\lambda^2 - \lambda^{-2} - 1) \quad (4)$$

where N is the average number of segments between consecutive junction points (i.e., between multiplets in this study).

Numerical evaluation of λ from eq 4 is listed in Table 1 for concentrations of 10 and 12 g/L and various shear rates. A clear increase of the chain extension is observed when the shear rate is increased, going from negligible extension in the Newtonian regime up to draw ratios of 2 in the shear-thickening zone. However, draw ratios are still rather moderate and not far within the non-Gaussian regime. Comparison between the two concentrations shows lower draw ratios for the more diluted solution for which shear thickening is also observed. Calculation of the draw ratios is based on the assumption that all chains contribute to the elasticity. In fact the dependence of the elastic modulus (G_0) on concentration shows that G_0 is systematically lower than νkT , where ν is the number of chains per unit volume.³ However, the difference steadily decreases as the concentration is increased. At 10 g/L, only $1/8$ of the chains are estimated to contribute to the elasticity whereas this fraction is somewhat higher ($1/4$) for 12 g/L. These values are only orders of magnitude taking into account the scatter in the data. Assuming that loops do not contribute to birefringence, the corresponding draw ratio of the extended chains has been computed and is listed in Table 1. Although relatively high, these extensions

are below the maximum draw ratio of these chains (≈ 30). However, the differences between the extensions at a given shear rate for the two solutions are reduced if the fraction of looped chains is taken into account.

It is surprising that the onset of shear thickening is observed at a higher shear rate when the concentration is decreased, since the characteristic relaxation time is independent of concentration. This behavior might be explained by an additional process responsible for shear thickening corresponding to the formation of bridges inside or between aggregates. Apparently, higher shear rates are required to induce this process as the concentration decreases. The existence of the large scale changes can also be understood by the long time required to reach steady state upon a even modest change in shear rate. It is however unlikely that very large aggregates are formed during the shear-thickening process since the transmitted intensity remains constant and no dichroism is detected.

Although the investigated systems are different, there is an apparent contradiction about the chain stretching when the birefringence measurements reported in this study are compared to the SANS experiments by Pedley et al.²⁰ The role of the loops which can even be the major component has to be considered. Indeed, loops do not contribute significantly to the birefringence, since their orientation requires shear rates higher than the reciprocal of the Rouse time, whereas they obviously contribute to neutron scattering, making the extended chains contribution more difficult to detect as suggested by Marrucci et al.¹⁹

Conclusion

The shear thickening of solutions of α,ω -lithium sulfonato polystyrene in toluene has been studied by flow birefringence measurements. The onset of the shear thickening is associated with a strong increase of birefringence upon increasing shear rate together with a sharp decrease in the orientation angle. This behavior has been discussed on the basis of chain stretching and from estimates of the chain extension ratio. It has been shown that the fraction of loops must be considered, leading-to-draw ratios on the order of 4 for the bridging chains which are actually stretched. This large stretching leads to highly elastic fluids undergoing a strong Weissenberg effect, which make this study at high shear rate difficult and the observation of the shear thinning regime almost impossible.

Acknowledgment. This work has been supported by the DIMAT joint program "Polymères Associatifs". Stimulating discussions with Dr. D. Durand and Dr. T.

Nicolai are gratefully acknowledged. R.J. is much indebted to the "Services Fédéraux des Affaires Scientifiques, Techniques et Culturelles" for general support to CERM in the frame of the "Pôles d'Attraction Inter-universitaires, PAI4/11".

References and Notes

- (1) (a) Schlick, S. *Ionomers: Characterization, Theory and Applications*; CRC Press Inc.: New York, 1996. (b) Tant, M. R.; Mauritz, M. R.; Wilkes, G. L. *Ionomers: Synthesis, Structure, Properties and Applications*; Blackie Academic & Professional: New York, 1997.
- (2) (a) Broze, G.; Jérôme, R.; Teyssié, P.; Marco, G. *Polym. Bull.* **1981**, *4*, 241. (b) Broze, G.; Jérôme, R.; Teyssié, P.; Gallot, B. *J. Polym. Sci., Polym. Lett. Ed.* **1981**, *19*, 415.
- (3) (a) Johannsson, R.; Chassenieux, C.; Durand, D.; Nicolai, T.; Vanhoorne, P.; Jérôme, R. *Macromolecules* **1995**, *28*, 8504. (b) Chassenieux, C.; Johannsson, R.; Durand, D.; Nicolai, T.; Vanhoorne, P.; Jérôme, R. *Colloids Surf. A* **1996**, *112*, 155.
- (4) Tant, M. R.; Wilkes, G. L.; Kennedy, J. P. *J. Appl. Polym. Sci.* **1991**, *42*, 523.
- (5) Bhargava, S.; Cooper, S. L. *Macromolecules* **1998**, *31*, 508.
- (6) Maus, C.; Fayt, R.; Jérôme, R.; Teyssié, P. *Polymer* **1995**, *36*, 2083.
- (7) Pedley, A. M.; Higgins, J. S.; Peiffer, D. G.; Rennie, A. R.; Staples, E. *Polym. Commun.* **1989**, *30*, 162.
- (8) Jérôme, R. in *Telechelic Polymers: Synthesis and Applications*; Goethals, E. J., Ed.; CRC Press: Boca Raton: FL, 1989; Chapter 11.
- (9) Peiffer, D. G.; Kaladas, J.; Duvdevani, I.; Higgins, J. S. *Macromolecules* **1987**, *20*, 1397.
- (10) Vanhoorne, P.; Maus, C.; Van der Bosche, G.; Fontaine, F.; Sobry, R.; Jérôme, R.; Stamm, M. *J. Phys. IV* **1993**, *3* (C8), 63.
- (11) Fuller, G. *Optical Rheometry of Complex Fluids*; Oxford University Press: New York, 1995.
- (12) Janeschitz-Kriegl, H. *Polymer Melt Rheology and Flow Birefringence*; Springer-Verlag: Berlin, 1983.
- (13) Kuhn, W.; Grun, F. *Kolloid Z.* **1942**, *101*, 248.
- (14) (a) Annable, T.; Buscall, R.; Ettelaie, R.; Whittlestone, D. *J. Rheol.* **1993**, *37*, 695; (b) Annable, T.; Buscall, R.; Ettelaie, R. *Colloids Surf. A* **1996**, *112*, 97.
- (15) Yekta, A.; Duhamel, J.; Brochard, P.; Adiwidjaja, H.; Winnik, M. A. *Macromolecules* **1992**, *26*, 1829.
- (16) Tam, K. C.; Jenkins, R. D.; Winnik, M. A.; Bassett, D. R. *Macromolecules* **1998**, *31*, 4149.
- (17) Van Egmond, J. W. *Curr. Opin. Colloid Interface Sci.* **1998**, *3*, 385.
- (18) Witten, T. A.; Cohen, M. H. *Macromolecules* **1985**, *18*, 1915.
- (19) Marrucci, G.; Bhargava, S.; Cooper, S. L. *Macromolecules* **1993**, *26*, 6483.
- (20) Pedley, A. M.; Higgins, J. S.; Peiffer, D. G.; Rennie, A. R.; Staples, E. *Polym. Commun.* **1989**, *30*, 162.
- (21) (a) Gurnee, E. F. *J. Appl. Phys.* **1954**, *25*, 1232. (b) Stein, R. S. *J. Appl. Phys.* **1961**, *32*, 1280.
- (22) Assuming uniaxial deformation around stretching direction would not change drastically the results. The dominant term in the right-hand side of eq 4 is $\lambda^2/5N$ in both cases.
- (23) Roe, R. J.; Krigbaum, W. R. *J. Appl. Phys.* **1964**, *35*, 2215.

MA991707C